The influence of Fe atom location on the electronic structure of $Ni_3Al_{1-x}Fe_x$: LMTO calculation and x-ray spectroscopy

2000 J. Phys.: Condens. Matter 12 2333

(http://iopscience.iop.org/0953-8984/12/10/317)

J. Phys.: Condens. Matter **12** (2000) 2333–2350. Printed in the UK PII: S0953-8984(00)10139-0

The influence of Fe atom location on the electronic structure of $Ni_3Al_{1-x}Fe_x$: LMTO calculation and x-ray spectroscopy

K Lawniczak-Jablonska, R Wojnecki and J Kachniarz

Institute of Physics, Polish Academy of Sciences, Aleja Lotników 32/46, 02 793 Warszawa, Poland

E-mail: jablo@ifpan.edu.pl

Received 7 December 1999

Abstract. The electronic structure of $Ni_3Al_{1-x}Fe_x$ ordered alloys was calculated using the *ab initio* self-consistent linear muffin-tin orbital method with the local density approximation. Two models of the preference in the site occupancy at the elemental cell were considered: (i) the Fe atoms substitute the Al atoms located at the corners of the fcc cube; (ii) the Fe atoms substitute the Ni atoms located at the faces of the cube and the appropriate number of Ni atoms is located at the cube corners. Changes in the 'raw' density of states distribution (DOS) for these two models were discussed and compared with the x-ray spectra. The magnetic moments calculated for the first model resemble the experimental data more than those calculated for the second one. The DOS distributions were calculated over a wide energy range in the valence as well as in the conduction band and projected on the constituent atoms separately for different symmetries of states. Such an approach allowed us to compare predictions of the theory with the appropriate x-ray spectra. In all collected x-ray spectra, one can find changes of characteristic features consistent with the changes observed in the calculated DOS under the assumption of the first model of site occupancy. The one-electron model was utilized in the spectrum interpretation. The performed studies indicated that it is the first model of Fe substitution that finds confirmation in the magnetic and x-ray investigations.

1. Introduction

One can observe that electronic devices are required to be more reliable, stable even in extreme conditions, small and light-weight. All this results in increasing expectations as to the properties of materials used in electronics. It has been shown that in binary compounds, certain ternary additives create significant improvements in the mechanical, electrical, magnetic and other properties of materials [1, 2]. Among the alloys of particular interest for commercial utility are still the Ni–Al-based alloys due to their high melting temperature, low density, good thermal stability and excellent oxidation resistance. However, the major barrier to application of Ni–Al is its low ductility and the tendency to fracture. Addition of Fe to nickel-rich Ni–Al alloys improves significantly their plasticity [3] and results in continuous interest in this class of materials. In order to help design alloys with improved mechanical and other properties, it is of fundamental importance to understand the changes in the electronic structure, i.e. the changes of the type of electron bonding for each constituent atom with change of composition. This motivated us to calculate the electronic structure of $Ni_3Al_{1-x}Fe_x$ alloys and to examine it by x-ray spectroscopy, the unique technique giving information on energy distribution of the density of states (DOS) projected on sites of selected atoms, separately for each symmetry of states. The ordered Ni_3Al crystallizes in a cubic structure of $L1_2$ type (γ' phase) where Al

0953-8984/00/102333+18$30.00

atoms occupy the cube corners and Ni atoms are located at the cube faces. The elements added to the Ni_3Al can be divided into three groups with respect to the site occupancy preference. These are ones which substitute for the Ni atoms, for Al atoms and randomly between both Ni and Al sublattices. It has been shown ([4, 5] and references therein) that Fe atoms in the stoichiometric Ni_3Al substitute predominantly Al sites but other suggestions are still discussed [6]. Nevertheless, it is commonly accepted that specific site occupancy originates rather from electronic properties of atoms than from simple size effects [7].

In the next section we present results of the DOS calculation performed over a wide energy range and projected on each constituent atom for two models of Fe site occupancy: (i) the Fe atoms substitute the Al atoms located at the corners of the fcc cube; (ii) the Fe atoms substitute the Ni atoms located at the face of the cube and appropriate number of Ni atoms are located at the cube corners. In section 3 the experimental details of the used spectrometers are collected. Due to the fact that appropriate spectra cover wide energy range, the experimental data were collected at four different facilities. In section 4, the comparison of the spectra with the predictions of the theory is presented. The paper is summed up in section 5.

2. Calculations and discussion

Several calculations of the DOS for binary Ni_3Al and Ni_3Fe compounds have been reported [8–14]. Total and partial densities of states, magnetic moments and elastic properties were considered therein. To determine influence of the addition of a third element, a cluster method has been applied [15]. To our best knowledge, no *ab initio* calculations for ternary $Ni_3Al_{1-x}Fe_x$ alloys have been reported.

Knowing the importance of iron addition to the physical properties of Ni_3Al alloy [1, 2], we concentrated on this element as a third component. The aim of the performed DOS calculations was to determine the influence of addition of Fe on the partial densities of states (PDOSs) around Ni and Al atoms in the cubic Ni_3Al ($L1_2$) compound under the assumption of two models of site occupancy: (i) the Fe atoms substitute the Al atoms located at the corners of the fcc cube; (ii) the Fe atoms substitute the Ni atoms located at the face of cube. The calculated distributions of DOS around different atoms were then directly compared with the x-ray spectra collected from $Ni_3Al_{1-x}Fe_x$ ordered alloys with various contents of Fe.

The well known method of linear combination of muffin-tin orbitals (LMTO) with the atomic spherical potential approximation (ASA) was used [16]. In this method the atomic potential is approximated by the muffin-tin spherical potential. The total volume of muffin-tin spheres around atoms in the elementary cell must be equal to the volume of that cell. The radii of the spheres are adjusted to obtain neutral atomic charge on each atom. This gives the most accurate description of metallic alloys ([6] and references therein) where ionic bonds are not formed.

The von Barth–Hedin approximation of the density functional was used. Calculations were made for 91 k-points in the irreducible part of the Brillouin zone (IBZ) of the bcc supercell. The accuracy of convergence of the total energy values was better than 5 μRyd.

The following models of the $Ni_3Al_{1-x}Fe_x$ bcc supercell were used in the performed calculations. The bcc superstructure was constructed from eight fcc cells. The base of the superstructure consists of 16 atoms. In the first model nickel atoms are placed in the face centres (filled circles in figure 1) and the aluminium and iron atoms occupy four different positions in the cube corners (empty circles with different filling—figure 1). Results of DOS calculations for $x = 0, 0.25, 0.5, 0.75, 1$, are presented in figures 2–4. This model introduces the artificial long-range order in Fe and Al positions. In real alloys, as have been shown by extended x-ray absorption fine structure (EXAFS) analysis performed on the same samples of alloys [4], the positions of Fe and Al are predominantly (77%) in cube corners but one

cannot completely exclude Fe or Al atoms in the position of Ni atoms [4, 17]. To examine the influence of the position of Fe atoms in the crystal cell on the DOS distribution and magnetic moments, we performed extra calculations with the Fe atoms placed at the face centres (filled circles in figure 1), and an appropriate number of Ni atom placed in the cube corners.

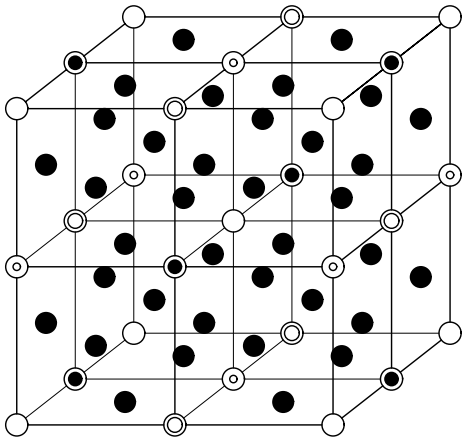

Figure 1. The bcc superstructure (formed by open circles empty inside). The superstructure consists of eight fcc cells. Solid circles on the fcc cells faces represent Ni atoms. Open circles with inside empty, small circle, large circle and filled circle represent four different positions at the cube corners occupied by Fe and Al atoms. For $x = 0$ all these positions are occupied by Al atoms: $x = 0.25$ the empty circles are occupied by Fe atoms; $x = 0.5$ additionally the empty circles with large circles inside are occupied by Fe atoms; $x = 0.75$ also the empty circles with large solid circles inside are occupied by Fe atoms; $x = 1.0$ all positions at the fcc cube corners are occupied by Fe.

Calculations were carried out for the lattice constant $a = 3.5638$ Å (6.735 407 Bohr units). However, x-ray diffraction measurements showed that the lattice constant depends on the Al/Fe ratio [4]. The observed changes of lattice constant were in the range of ± 0.004 Å and did not influence the DOS shape, as was checked by separate calculations and in particular cannot influence our comparison with x-ray spectra.

The calculated spin-up and spin-down DOSs for the superstructure presented in figure 1, projected on Ni, Fe and Al atoms are shown in figures 2, 3 and 4, respectively. The DOS scale is the same for spin-up and spin-down states in all presented plots. Let us discuss the trends in the shape of partial DOS energy distribution at the particular atom after introducing the Fe atoms in the ordered Ni_3Al alloy.

In figure 2, the nickel s, p spin-up and down DOS in the energy range from -10 eV to +20 eV are presented. The d states of Ni are localized close to the Fermi level, therefore, only the energy range from -5 eV to 2 eV is shown with an expanded scale to enhance the observed changes which would be not visible in the same scale as used for s and p states (notice also the change in the DOS scale). The number of spin-up and down states with s and p symmetry around the Ni atoms is roughly the same for all contents of Fe. There appear, however, some changes in the shape of spin-up and down states when the concentration of Fe atoms increases up to 2 atoms per unit cell ($x = 0.5$). The situation is different for d states. In the case of Ni_3Al, a clear difference is seen in the conduction band when the d spin-down states dominate and are gathered into two peaks close to the Fermi level (FL) and around 1.1 eV. Addition of Fe atoms significantly changes the d-state distribution. The states become less localized and their maximum shifts away from the FL, and for the Ni_3Fe alloy the states cover a distance

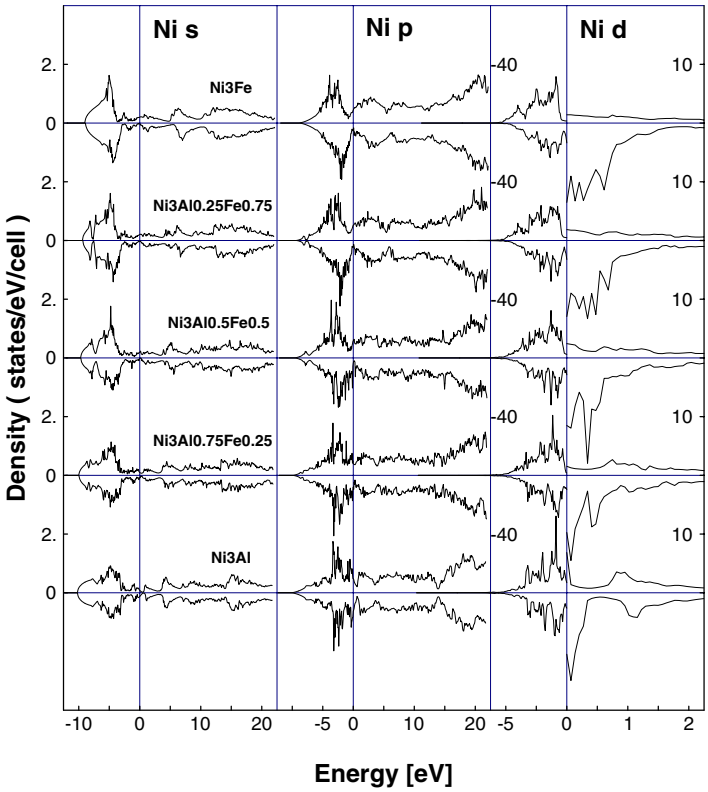

Figure 2. Partial densities of states for Ni in $Ni_3Al_{1-x}Fe_x$ ($x = 0, 0.25, 0.5, 0.75, 1$). DOS scale for Ni s and Ni p is on the left side of the plot, DOS scale for Ni d: below E_f is in the plot, above E_f is on the right side of the plot. Both spins have the same scaling for all the plots.

from the FL up to 1 eV. In the valence band, the d spin-up states dominate. One can notice that a sharp maximum of spin-up d states in Ni_3Al disappears after introducing the Fe atoms. Summarizing, one can state that introduction of Fe atoms influences mostly the Ni d states and causes delocalization of the sharp d-state peaks in the valence and conduction bands.

In figure 3, the iron spin-up and down DOSs in the energy range from -10 eV to +20 eV for s and p symmetry and from -5 to +2 eV for d symmetry are presented. As could be expected, the number of states in all parts of the plot is decreasing with decrease of the number of Fe atoms in the unit cell. For s states, the differences between spin-up and down states are small but noticeable in all four compounds. The spin-up DOS below the FL forms a dominant peak at -5 eV but with decrease of Fe content, the sharp peak disappears and several additional local peaks are formed. A similar situation is found above the FL. The s conduction states form a peak at 6 eV and a broad band from 10 eV to 20 eV for Ni_3Fe. With decrease of the Fe content, the density of states shows a tendency to form several localized peaks. In the p-state distribution, a close similarity can be seen between spin-up and spin-down states but the highest peak is formed by the spin-down states for $x = 0.75$. The peak of DOS in the valence band is located around -2.5 eV and the DOS minimum is close to the FL. Similarly as for Ni, the Fe d states show the most pronounced difference between spin-up and spin-down states. Below the Fermi level, the majority are spin-up states and the states are gathered into two groups (sharp peak close to the FL and other states) for Ni_3Fe, and into three groups for

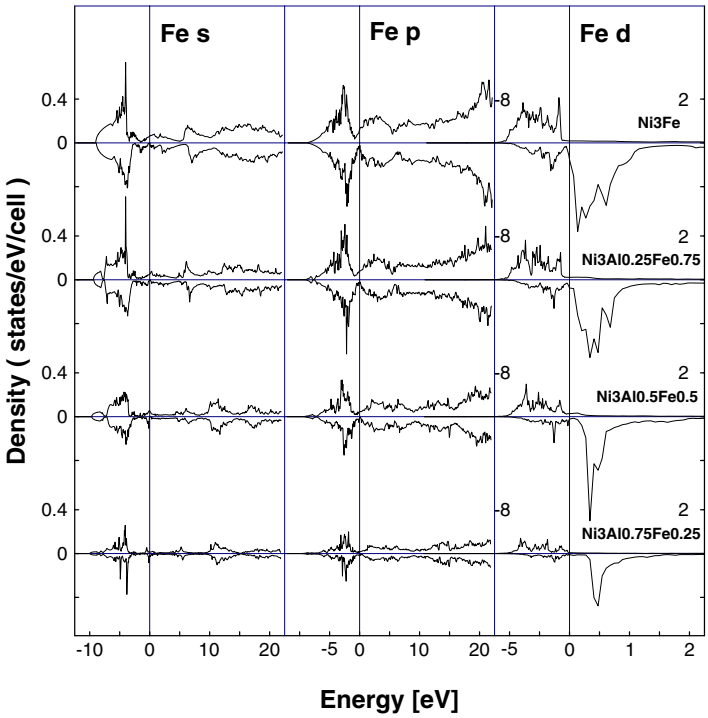

Figure 3. Partial densities of states for Fe in $Ni_3Al_{1-x}Fe_x$ ($x = 0.25, 0.5, 0.75, 1$). DOS scale for Fe s and Fe p is on the left side of the plot, DOS scale for Fe d: below E_f is in the plot, above E_f is on the right side of the plot. Both spins have the same scaling for all the plots.

other alloys. A very small Fe DOS value at the FL is also worth noting. Above the FL, the majority of states are spin-down ones. With decrease of the number of Fe atoms, the width of the spin-down DOS peak decreases and the distance between this peak and the FL increases. Summarizing the observed tendency in the PDOS around the Fe atoms, one can state that the decreasing content of Fe atoms results in an increase of the distance between Fe atoms in the crystal and decrease of the Fe electron wavefunction overlapping. This usually leads to increasing localization of the DOS in the energy space which is clearly seen in figure 3.

In figure 4, the aluminium s, p and d spin-up and down DOS distributions in the energy range from −10 eV to +20 eV are presented. For states of different symmetries, the spin-up and down plots are almost the same. There are no differences in the d Al states of the kind observed at the Ni and Fe atoms. Hence, one can say that Al states do not influence significantly the magnetic properties of the considered alloys. Similarly as observed for the Fe DOS, a decrease of Al content in the alloys leads to an increase of localization of electron states in the energy space and states show a tendency to gather into separated peaks, which is particularly well seen in the valence band of s electrons. The p electrons in the valence band of Ni_3Al exhibit one dominant peak around −3.5 eV. This peak spreads out into several peaks after introducing the Fe atoms.

Summarizing, the DOS distribution around Ni atoms, which dominate in the total DOS, shows the tendency to be more uniformly distributed in the energy space in the valence as well as in the conduction band after introducing the Fe atoms to the ordered Ni_3Al alloy. The isotropic distribution of the electron charge in the interatomic bond can result in an increase of the alloy plasticity. The DOS distributions around Fe and Al atoms show a tendency to gather

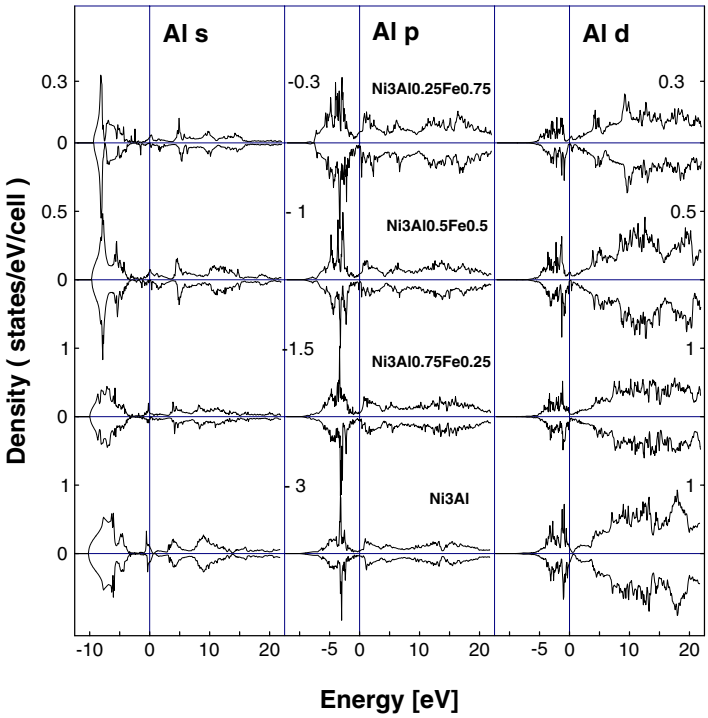

Figure 4. Partial densities of states for Al in $Ni_3Al_{1-x}Fe_x$ ($x = 0, 0.25, 0.5, 0.75$). DOS scales for Al s and Al p are on the left sides of the plots, respectively, DOS scale for Al d is on the right side of the plot. The scale is shown for spin up only; both spins have the same scaling for all the plots.

into more localized peaks when the numbers of particular atoms decrease, but these peaks are spread over a wide energy range.

In table 1, the average magnetic moment per atom (μ_B/atom) as well as the magnetic moment located at each i atom (μ_i) resulting from calculations performed for two models of Fe location are collected together with the experimental data from [18–20]. The average magnetic moment per atom is rapidly increasing with increase of the Fe atom number per unit cell. The magnetic moment located at the Fe atoms does not change much for any of the considered compounds; only for the alloy with equal number of Al and Fe atoms is it significantly smaller than for other alloys. The moment located at the Al atom has opposite direction and is much smaller than that located at Fe and Ni. The most surprising is the increase of the magnetic moment located at the Ni atom extorted by the increasing number of Fe in the unit cell. Therefore, the increase of magnetic moment in the considered alloys is not only due to the increase of the number of Fe atoms per unit cell but also to the increase of magnetic moment induced at the Ni atoms. Similar phenomena have been reported for $(Fe_{1-x}Ni_x)_4N$ for Ni atoms occupying the face-centre sites [21]. The calculated mean magnetic moment per atom (table 1) corresponds excellently to the experimental results reported by Efthimiadis and Tsoukalas [18, 19]. In the case of the Fe atom being located at the cube faces and Ni shifted to the cube corner (b), the magnetic moment calculated per Ni (the mean value for two non-equivalent Ni atoms) and Fe atoms is smaller than in the case where Fe atoms were placed in the cube corners (a). The average magnetic moments resulting from model (a) are more consistent with the reported experimental data.

Table 1. The $Ni_3Al_{1-x}Fe_x$ ($x = 0, 0.25, 0.5, 0.75, 1$) magnetic moments μ_i located at each atom as well as average magnetic moment per atom in unit cell for two models of Fe atoms location in the elemental cell: (a) at the cube corners; (b) at the face centres. In the model (b) two non-equivalent positions of Ni atoms are reported: the first at the cube corners, the second at the face centres. Magnetic moments are in Bohr units. Experimental data from [19, 20].

Alloy		μ_{Ni}	μ_{Al}	μ_{Fe}	μ_B/atom	μ_B/atom (exp.)
Ni_3Al	(a)	0.25	−0.03		0.18	0.07 [19], 0.24 [20]
$Ni_3Al_{0.75}Fe_{0.25}$	(a)	0.40	−0.05	2.67	0.45	0.46[a] [19]
	(b)	0.66, 0.37	−0.05	2.35	0.43	
$Ni_3Al_{0.5}Fe_{0.5}$	(a)	0.47	−0.07	2.53	0.66	0.69 [19]
	(b)	0.44, 0.42	−0.08	2.32	0.60	
$Ni_3Al_{0.25}Fe_{0.75}$	(a)	0.59	−0.07	2.61	0.93	0.93[a] [19]
	(b)	0.64, 0.56	−0.10	2.49	0.91	
Ni_3Fe	(a)	0.70	—	2.64	1.18	1.17 [19]
	(b)	0.70, 0.70	—	2.64	1.18	

[a] The experiment was performed for $\Delta x = 0.1$ therefore for other composition the extrapolated value was used for comparison.

3. Experiment

The $Ni_3Al_{1-x}Fe_x$ samples with $x = 0$, 0.2, 0.55, 0.7, 1.0 were melted from 5 N Al, 4 N Ni and 4 N Fe. The alloys were then cast in a high-frequency furnace under Ar flow and rapidly solidified. The samples were annealed for one week at a temperature below the $L1_2$ phase boundary, in order to obtain maximum homogeneity and long-range ordering. Samples cut in the form of flat 1 mm thick plates were used for x-ray measurements.

X-ray spectroscopy is the unique technique providing direct information on the DOS distribution over a wide energy range in the valence band (emission spectroscopy) and in the conduction band (absorption spectroscopy). Proper adjusting of the energy of the analysed x-ray radiation allows us to monitor separately the DOS distribution around each constituent atom. Additionally, the electron transition rules separate states of different symmetry [22]. Therefore, to check the reliability of performed calculations and choose the proper model of Fe atom location in the elemental cell, we decided to collect appropriate spectra and compare them with theoretical predictions.

The resonantly excited Ni Lα emission spectra were measured at the HASYLAB, Hamburg, Germany, at the beamline BW3 using a grazing-incidence spectrometer in a Rowland mounting [23] with a position-sensitive multi-channel plate detector. A blazed holographic grating of 5 m radius with 1200 lines mm^{-1} was used in second order of diffraction. In the investigated range of energy, the overall energy resolution was close to 1 eV. To avoid the influence of the Lβ line, the spectra were excited in a resonance mode by the radiation of an energy (856 eV) lower then the binding energy of the $2p_{1/2}$ electron level (870.0 eV).

Lα emission spectra of Fe and Kβ emission spectra of Al were measured using the wavelength-dispersive mode of an electron microprobe. The energy of the electron beam was set on 7 keV and 10 keV, respectively. A TAP crystal was used to measure both spectra. Due to wide slits in the spectrometer, the energy resolution was of the order of 1 eV.

The Lα absorption spectra of Ni, Fe and Al were recorded at the Advanced Light Source, Lawrence Berkeley National Laboratory, Berkeley, CA, at the beamline 6.3.2 [24] using the total photocurrent technique of signal detection. The L edges of Ni and Fe were measured using a 1200 lines mm^{-1} plane grating with resolutions 0.45 eV and 0.35 eV (30 μm slit), respectively for Ni and Fe. The L edge of Al was measured using a 300 lines mm^{-1} grating with the resolution of 0.05 eV (slit 50 μm).

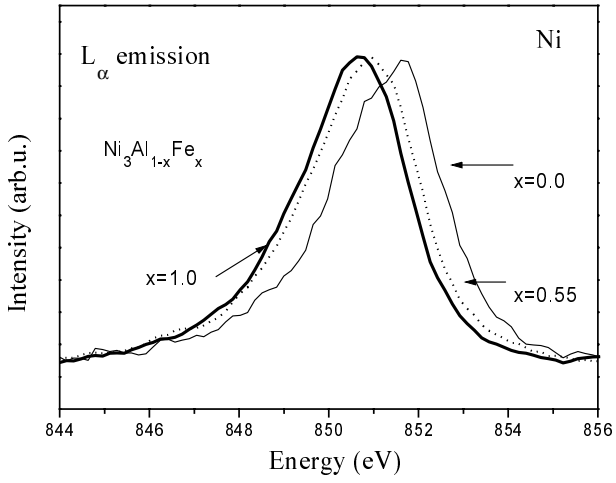

(a)

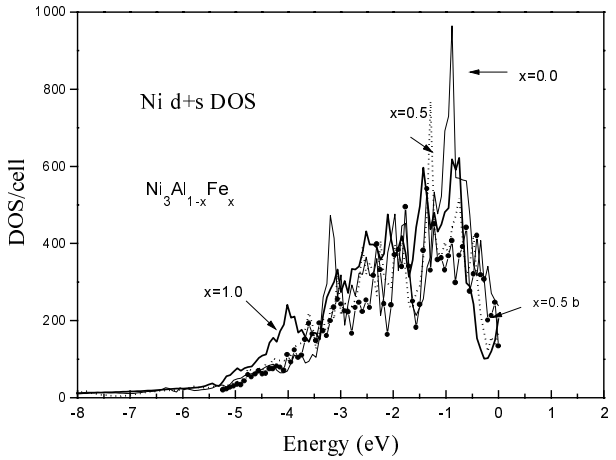

(b)

Figure 5. (a) Resonantly excited x-ray emission Lα spectrum of Ni atoms in Ni_3Al (thin line), Ni_3Fe (thick line) and $Ni_3Al_{0.45}Fe_{0.55}$ (dotted line). (b) The d + s valence DOS around the Ni atoms in Ni_3Al (thin line), Ni_3Fe (thick line), $Ni_3Al_{0.5}Fe_{0.5}$ (dotted line for Ni atoms located at the cube face $x = 0.5$ and solid-circle line for two Ni atoms located at the corners—$x = 0.5$ b). (c) The d + s valence DOS broadened by the Gaussian (FWHM 1 eV) and by the Lorentzian (FWHM 0.8 eV) around the Ni atoms in Ni_3Al (thin line), Ni_3Fe (thick line), $Ni_3Al_{0.5}Fe_{0.5}$ (dotted line for Ni atoms located at the cube face $x = 0.5$ and solid-circle line for two Ni atoms located at the corners—$x = 0.5$ b).

The K edges of aluminium were recorded at the SuperAco ring, station SA32 at LURE, Orsay, France. The measured quantity was the total photocurrent from the sample. A beryllium crystal monochromator provided the spectral range of 0.8–3 keV with 0.2 eV energy resolution at the K edge of Al. The measurements of Ni and Fe K edges were performed at the bending magnet station E4, HASYLAB, equipped with the Si(111) double crystal monochromator. The proper choice of slits resulted in the resolution of 0.6 eV.

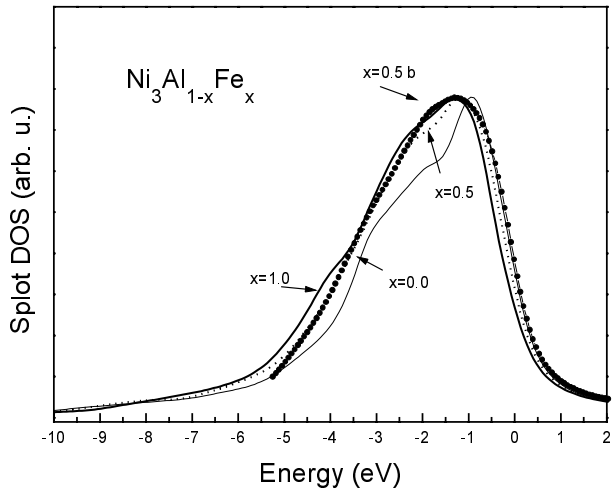

(c)

Figure 5. (Continued)

4. Comparison of the measured spectra with the DOS distributions

The measured x-ray Lα emission spectra of Ni are presented in figure 5(a). For clarity of presentation, only spectra for $x = 0.0$, 0.55 and 1.0 are shown. The spectra for alloys of compositions between the indicated ones follow the observed tendency. Due to the lack of the intensity calibration, the intensities of all presented spectra were normalized to the maximum of a spectrum peak. The Lα spectra are created due to electron transition from the 3d and 4s valence state of an atom to a hole at the $2p_{3/2}$ core level. The hole is created by x-ray photons with an energy slightly exceeding the binding energy of $2p_{3/2}$ electrons to avoid the influence of the excitation of $2p_{1/2}$ electrons on the shape of the high energy side of the spectrum. In the discussion, we use the one-electron approximation. This means that the presence of a hole either at the valence or at the core levels does not influence the DOS distribution. This assumption is generally true in the case of metals and metallic alloys ([25] and references therein) but 3d metals can be exceptions. Particularly well known is the influence of the electron correlation effect (many body effect) on the shape of the Ni spectra but, as shown by one of the authors (KL-J) [26], this effect in much less important in the case of Ni alloys. Nevertheless, in the presented alloys the Fe atoms (also a 3d metal) are added and the same correlation effects still can narrow the observed spectra, as indeed can be noticed in figure 5(c) where the DOSs were broadened by the spectrometer function approximated by a Gaussian with the full width at half maximum (FWHM) equal to 1 eV and by the Lorentzian with FWHM equal to 0.8 eV to account for the initial and final state lifetimes. In spite of the fact that emission spectra are narrower than the broadened DOS one can observe the same changes in the 'raw' DOS and in the DOS after convolution and in the measured spectra with the addition of Fe atoms. As we do not study the correlation effects in this paper but the changes introduced by addition of Fe atoms to the Ni_3Al alloy, we neglect the broadening of the calculated DOS by the spectrometer and life-time broadening functions, knowing from previous studies [27, 28] that it only smooths the DOS features and cannot add any structure absent in the 'raw' DOS. An additional factor which can influence the spectra shape is the transition cross-section, which is not easy to account for but usually changes the relations between the intensity of particular maxima.

In figure 5(a), one can see that the spectrum of Ni_3Al is shifted about 1 eV toward higher energy as compared to the spectra of Ni_3Fe alloy, and is narrower at the maximum than the other spectra. These changes are in agreement with the results of DOS calculations (figure 5(b) and 5(c)) where the sharp peak located at -1 eV in Ni_3Al, after introducing Fe atoms, disappears. The states close to the FL shift about 0.5 eV in the direction of low energy, which is less than in the spectra but the correlation effect can additionally increase this shift. The widths of the spectra (and DOS) at the bottom remain the same but in the case of Ni_3Al, there are fewer states located at the band low energy tail. The substitution of Fe atoms into the positions of Ni atoms gives the DOS distribution marked as (b) for $x = 0.5$. The change in the position of Fe atoms results in increasing of the states density close to the FL for the $x = 0.5$ (solid-circle line) and disappearing of the shift observed between spectra of Ni_3Al and ternary alloys. The difference in the intensity distribution for $x = 1.0$ and $x = 0.5$ around -2 eV disappears for model b, which is in disagreement with the spectra. Therefore, the registered spectra support the first model of Fe atom location.

In figure 6(a), the L_3 absorption edges of Ni in the same alloys are presented. Due to the dipole selection rules, the L_3 absorption spectrum is created during the electron transition from the $2p_{3/2}$ level to the d + s-electron states in the conduction band. The presence of Fe atoms leads to decrease of the intensity of the structure located about 1.2 eV from the spectrum maximum. This structure is a result of the electron state peak located about 1.2 eV from the FL in Ni_3Al (figure 6(b)). The natural width of the $2p_{3/2}$ level smoothed out the minimum separating this peak from the maximum of DOS at the FL and manifested itself in this enhanced structure. After introducing Fe atoms, the DOSs are more uniformly distributed and the number of states at this peak decreases. One can notice that at the energy 2 eV states of ternary alloy are slightly higher than Ni_3Fe but below 1 eV states from Ni_3Fe dominate which is also seen in the spectra. Similarly as for valence states, the DOS distributions calculated under the assumption of the second model (b) of Fe atom substitution for $x = 0.5$ are, for comparison, shown by the solid-circle line. This DOS is very similar to the DOS for model (a). Therefore, the changes observed in the d + s Ni conduction states for the two considered models cannot produce any pronounced structure in spectra which would allow us to exclude one of them. The main influence of Fe on the Ni d + s-electron states distribution found in the experimental spectra and confirmed by calculations is that the d electrons around the Ni atoms become more uniformly distributed in valence as well as in conduction bands and the sharp peaks observed in Ni_3Al are smoothed out and shifted away from the FL.

Due to the dipole selection rule, close to the binding energy of Ni 1s electrons (8333 eV) one can observe the Ni K absorption edge which contains information on the energy distribution of p-symmetry states in the conduction band around the Ni atom (figure 7). The shapes of the K edges for all atoms are additionally affected by continuous scattering on the atomic potential, which is the reason for the continuous increase of the intensity with increase of the x-ray radiation energy near the edge, observed in all registered K edges. Nevertheless, the main features of the calculated 'raw' DOS distributions (A, B, C) well manifest themselves in the structure of spectra. With the increase of Fe content, the intensity of the maximum marked as C increases. A similar increase of the number of states can be seen in the p-DOS distribution shown in the lower part of figure 7 in the appropriate energy scale. This effect is also seen in the DOS calculated under the assumption of the second model. Therefore, from consideration of the K edges, we cannot exclude either of the two models.

In the valence band of Al, as can be judged from figure 4, the p-symmetry states dominate. Looking at the changes of the p-electron distribution around the atom monitored in the Kβ emission spectra, one can notice (figure 8(a)) that after introducing Fe in the ordered Ni_3Al, the centre of gravity of the spectra shifts away from the FL and the shape of the spectrum does

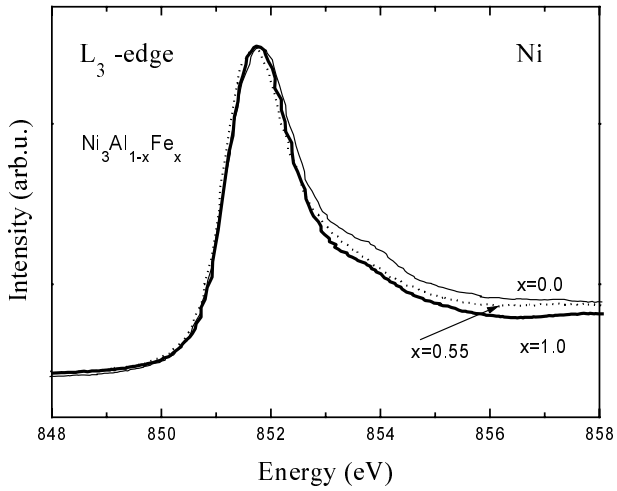

(a)

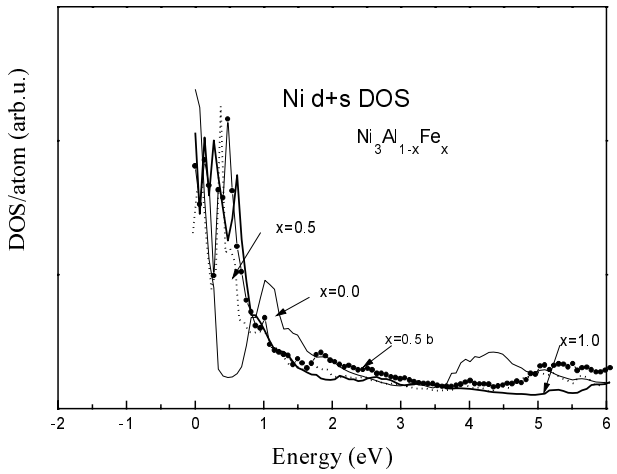

(b)

Figure 6. (a) L_3 absorption edge of Ni atoms in Ni_3Al (thin line), Ni_3Fe (thick line) and $Ni_3Al_{0.45}Fe_{0.55}$ (dotted line). (b) The d + s conduction DOS around the Ni atoms in Ni_3Al (thin line), Ni_3Fe (thick line) and $Ni_3Al_{0.5}Fe_{0.5}$ (dotted line for Ni atoms located at the cube face $x = 0.5$ and solid-circle line for two Ni atoms located at the corners—$x = 0.5$ b).

not change much; only at the bottom of spectra can some increase of the intensities be noticed. In figure 8(b), the p valence electron states around Al atoms indicate the same tendency. Similarly as in the case of spectra, the DOSs were normalized relative to the element content. The DOS located in Ni_3Al at the sharp peak around -3 eV, after introducing Fe spreads over an energy range from -5 to -2 eV and the number of states at the low energy side, particularly around -4.5 eV, noticeably increases in the alloy with $x = 0.5$, and is higher than in the alloy with $x = 0.75$ as can be also observed in the emission spectra. We did not observe any changes at the high energy side of spectra following the DOS increase around -2 eV. The increase of DOS started at -1.5 eV from the FL, not as in the case of Ni atoms just at the FL. The

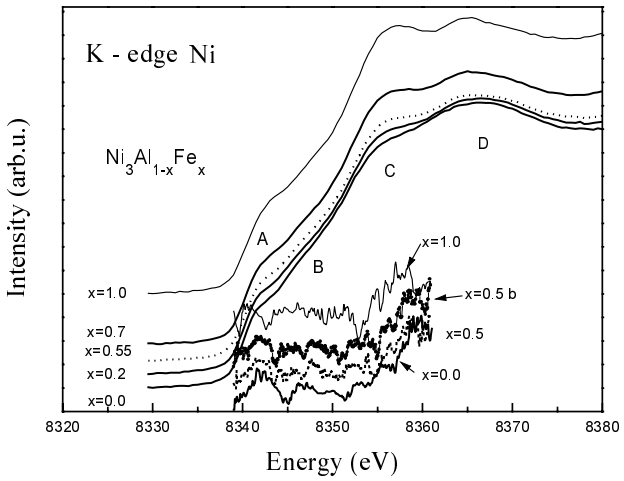

Figure 7. K absorption edge of Ni atoms in $Ni_3Al_{1-x}Fe_x$ ($x = 0.0$, 0.2, 0.55, 0.7, 1) and the p states at the conduction band around the Ni atoms for $x = 0.0$ (thick line), $x = 1.0$ (thin line) and $x = 0.5$ (dotted line for Ni atoms located at the cube face and solid-circle line for two Ni atoms located at the corners—$x = 0.5$ b). Spectra and DOS plots are shifted along the y-axis for clarity of presentation.

convolution with broadening functions smeared this increase, particularly in the presence of the sharp peak (−3 eV) in Ni_3Al. The DOS distribution for the second model (line with solid circles) differs in some details but these differences are too small to produce any pronounced structure in the spectra. The Ni and Fe atoms are very similar, therefore it is not surprising that Al atoms do not 'feel' change in the near neighbourhood.

The Al p states in the conduction band can be observed in the Al K edge. The K edges together with the plot of the appropriate 'raw' p-DOS distributions in the same energy scale are presented in figure 9(a). The first pronounced minimum of DOS at the distance of 5 eV from the FL (1562 eV at the scale of K edge) well corresponds to the first wide minimum of the spectra. With addition of Fe atoms, this minimum becomes broader and, for the alloy with lowest content of Al ($x = 0.7$), extends up to 1564 eV. If we look at the DOS distributions, we notice that this is caused by disappearance of the DOS peak located in Ni_3Al at 6 eV from the FL (1563 eV). In the DOS for alloy with $x = 0.5$, a deep minimum is located at this position and a peak of states around 9 eV (1566 eV) is formed. In the spectra, gradual increase of intensity around 1567 eV can be observed. Another well pronounced change in the DOS is the disappearance of the minimum located in Ni_3Al at 15.5 eV from the FL (1572.5 eV). This effect can also be observed in the spectra where gradual smoothing of the minimum at 1573.5 eV with increase of Fe content is well seen. The DOS distribution for the second model of site occupancy (b), up to the energy 1572, is very similar to the DOS for the first model. For the higher energy, some differences can be noticed. The maximum close to the energy 1575 eV where a deep minimum appears in the spectra is the most pronounced difference which is in favour of the first model.

The plots of d + s-DOS distribution and the Al $L_{2,3}$ edges are collected in figure 9(b). The distance between the 2p spin–orbit doublet in Al atom is equal to 0.5 eV, therefore one cannot resolve the structure consisting of transitions from these two orbitals, but this can cause an extra broadening of the spectra and can add an extra structure to them. The structure marked A is well manifested in the spectra. We did not observe a shift in the energy position of peak B in the spectra. This peak is located at the energy range where the atomic absorption increases. This, together with superposition of contributions from the two orbitals, may be responsible

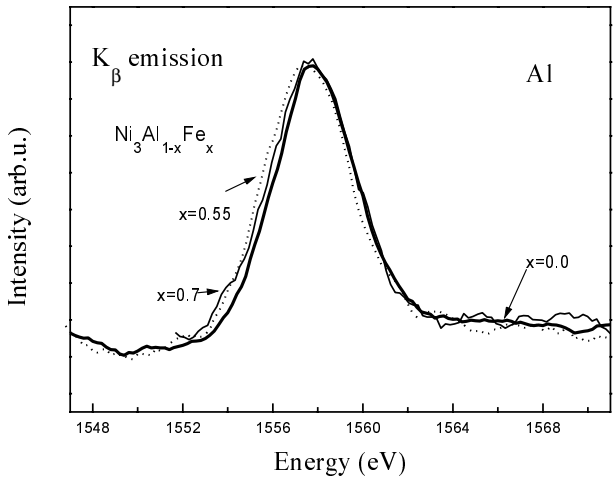

(a)

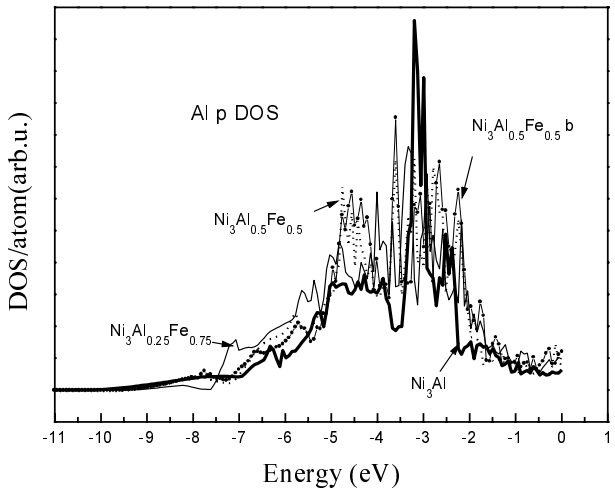

(b)

Figure 8. (a) X-ray emission Kβ spectrum of Al atoms in Ni_3Al (thick line), $Ni_3Al_{0.45}Fe_{0.55}$ (dotted line) and $Ni_3Al_{0.3}Fe_{0.7}$ (thin line). (b) The p valence DOS around the Al atoms in Ni_3Al (thick line), $Ni_3Al_{0.5}Fe_{0.5}$ (dotted line for Ni atoms located at the cube face and solid-circle line for two Ni atoms located at the corners—$Ni_3Al_{0.5}Fe_{0.5}$ b) and $Ni_3Al_{0.25}Fe_{0.75}$ (thin line).

for smearing of this effect. In contrast, the difference in the amount of DOS around the peaks C and E in ternary and binary alloys is well seen. The origin of the structure D in the spectra is not clear because it is located just at the minimum of the DOS of ternary alloys. However, some structure in the Ni_3Al DOS distribution located close to that position can be distinguished. Nevertheless, repeating of the DOS structure by the $2p_{1/2}$ orbital cannot be excluded. Due to the fact that this structure appears in the energy range where the atomic absorption decreases, it is difficult to make decisive statements here. Two minima, located at 84 eV and 88 eV, correspond reasonably well with the minima at the DOS structure but additional structure of DOS is not resolved in the spectra. There are no remarkable differences of DOS distributions

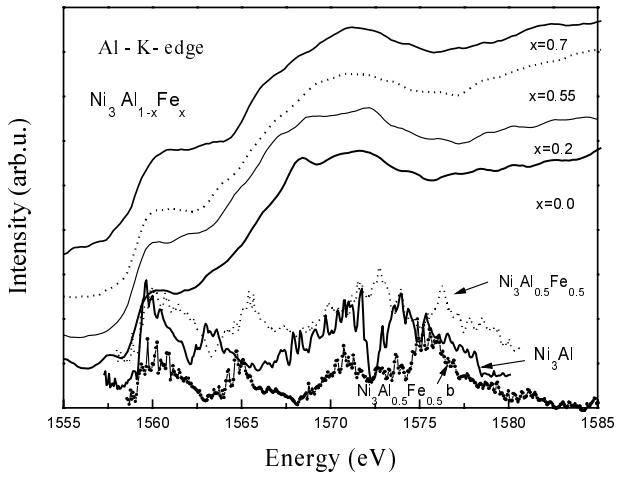

(a)

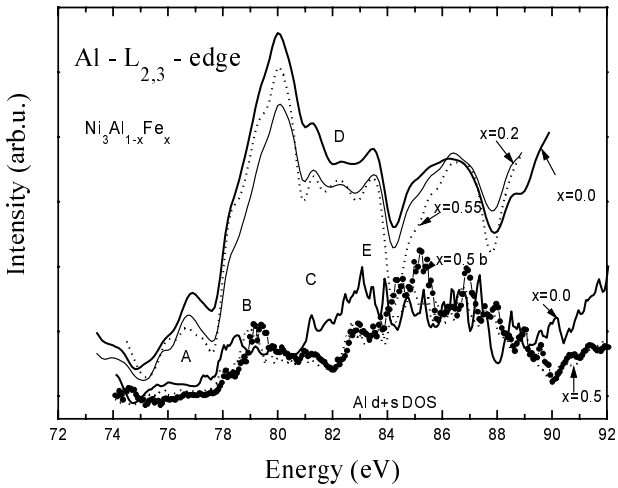

(b)

Figure 9. (a) K absorption edge of Al atoms in $Ni_3Al_{1-x}Fe_x$ and p conduction DOS around the Al atoms in Ni_3Al (thick line) and $Ni_3Al_{0.5}Fe_{0.5}$ (dotted line for Ni atoms located at the cube face and solid-circle line for two Ni atoms located at the corners—$Ni_3Al_{0.5}Fe_{0.5}$ b). (b) $L_{2,3}$ absorption edge of Al atoms in Ni_3Al (thick line), $Ni_3Al_{0.8}Fe_{0.2}$ (thin line) and $Ni_3Al_{0.45}Fe_{0.55}$ (dotted line).The d + s conduction DOS around the Al atoms in Ni_3Al (thin line) and $Ni_3Al_{0.5}Fe_{0.5}$ (dotted line for Ni atoms located at the cube face $x = 0.5$ and solid-circle line for two Ni atoms located at the corners—$x = 0.5$ b).

between the two models of Fe atom occupancy.

Finally, let us look at the DOS around the Fe atoms. The valence d + s states (figures 10(a) and 10(b)) show a tendency opposite to that of Ni and p states of Al. The centre of gravity of spectra shifts to the direction of higher binding energy (to the FL). Some extra states appear at the minimum of DOS close to the FL, and the bottom of DOS is shifted about 0.5 eV (for $x = 0.5$) in the direction of the FL. The same tendency is observed in the Lα emission spectra of Fe and even more pronounced in the DOS calculated for the second model (solid-circle

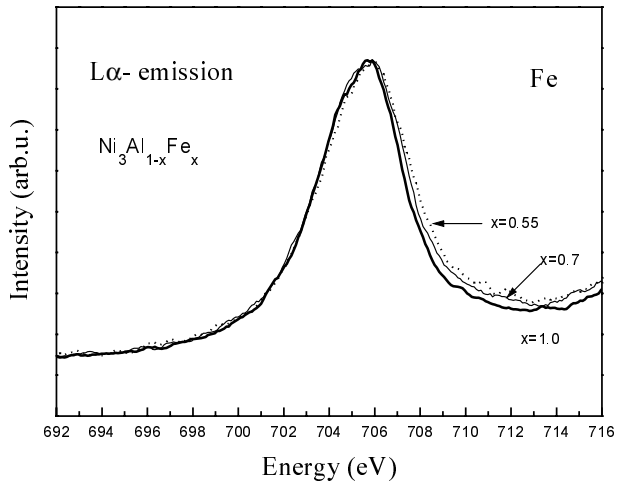

(a)

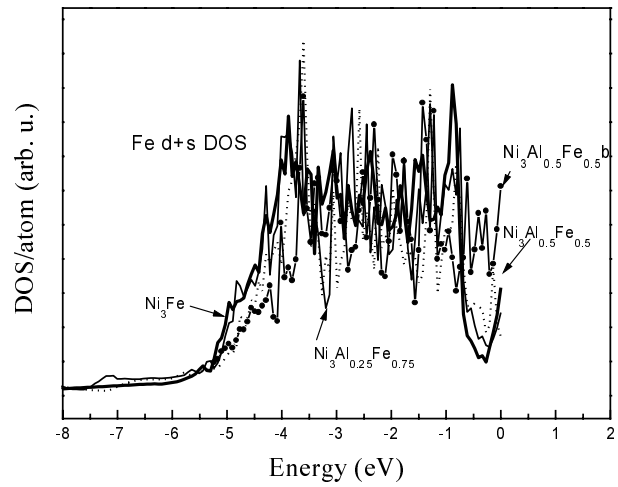

(b)

Figure 10. (a) X-ray emission Lα spectrum of Fe atoms in Ni_3Fe (thick line), $Ni_3Al_{0.3}Fe_{0.7}$ (thin line) and $Ni_3Al_{0.45}Fe_{0.55}$ (dotted line). (b) The d + s valence DOS around the Fe atoms in Ni_3Fe (thick line), $Ni_3Al_{0.25}Fe_{0.75}$ (thin line) and $Ni_3Al_{0.5}Fe_{0.5}$ (dotted line for Ni atoms located at the cube face and solid-circle line for two Ni atoms located at the corners—$Ni_3Al_{0.5}Fe_{0.5}$ b).

line). Keeping in mind that these spectra were measured by conventional spectroscopy where the presence of the Lβ line can influence the high energy side of spectra, in the case when the second model is true, we should observe a more pronounced effect in x-ray emission.

Nevertheless, the d + s conduction states shift in ternary alloys away from the FL and are localized at the distance of 0.5 eV from the FL (figure 11(b)). The localization of these states increases in ternary alloys. Although the L_3 absorption edge is broadened by the natural width of the $2p_{3/2}$ orbital and the spectrometer function, the same tendency is seen in the spectra (figure 11(a)). The spectrum for $x = 0.2$ is narrowed and shifted in the direction of high energy. In both spectra, for $x = 1.0$ and $x = 0.5$, the high energy shoulder is shown where

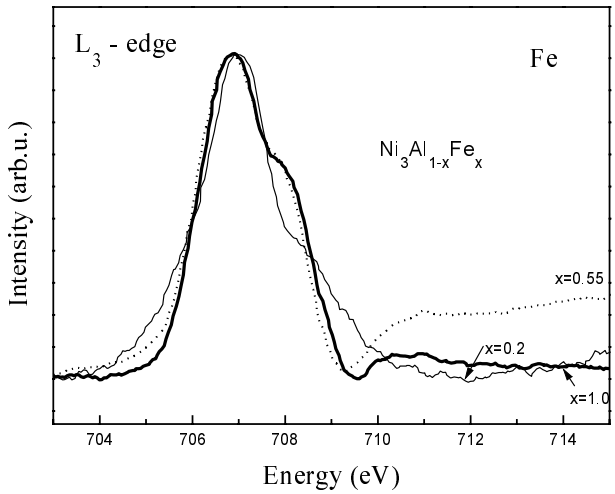

(a)

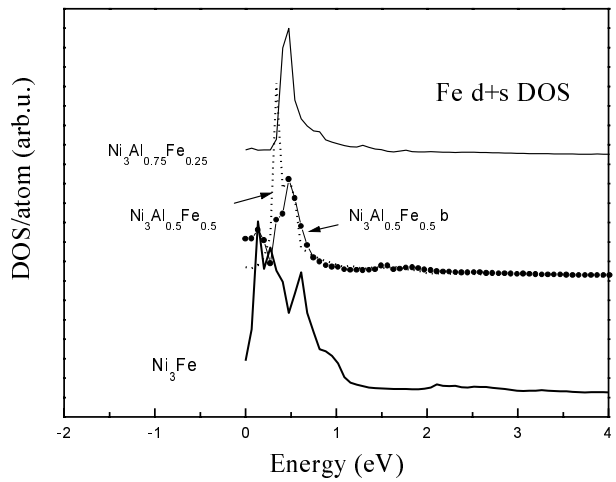

(b)

Figure 11. (a) L_3 absorption edge of Fe atoms in Ni_3Fe (thick line), $Ni_3Al_{0.8}Fe_{0.2}$ (thin line) and $Ni_3Al_{0.45}Fe_{0.55}$ (dotted line). (b) The d + s conduction DOS around the Fe atoms in Ni_3Fe (thick line) and $Ni_3Al_{0.5}Fe_{0.5}$ (dotted line for Ni atoms located at the cube face and solid-circle line for two Ni atoms located at the corners—$Ni_3Al_{0.5}Fe_{0.5}$ b) and $Ni_3Al_{0.25}Fe_{0.75}$ (thin line).

structure can be seen related to that in DOS distribution. We did not, however, resolve differences in the main peak positions and the spectrum widths as the DOS distribution suggests. The DOS distribution for the second model of site occupancy differs significantly and the low energy shoulder is formed which is not observed in the spectra. Therefore, the L emission and absorption spectra give evidence in favour of Fe occupancy of the corners at the fcc cube.

The p conduction states are presented in figure 12 (bottom of the figure) together with the K absorption edge of Fe. The features marked as A, B, C, D in the p-DOS distribution find their reflections in the features of K edges. With the increasing content of Al, the structure B increases, and increase of intensity is seen in the related part of the spectra. Due to the fact

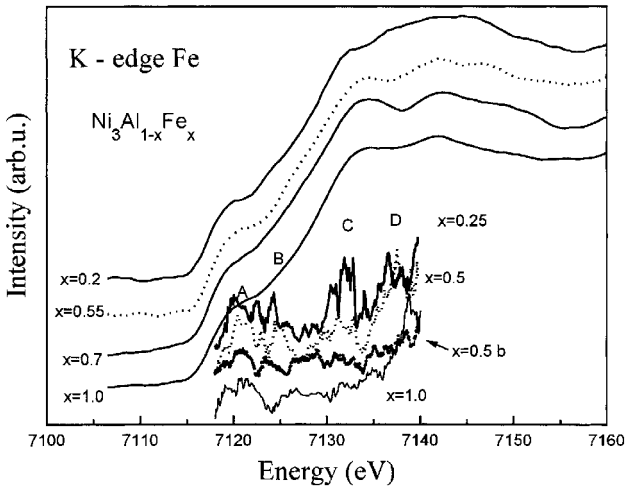

Figure 12. K absorption edge of Fe atoms in $Ni_3Al_{1-x}Fe_x$ ($x = 0.2, 0.55, 0.7, 1$) and the p states at the conduction band around the Fe atoms for $x = 0.25$ (thick line), $x = 1.0$ (thin line) and $x = 0.5$ (dotted line for Ni atoms located at the cube face and solid-circle line for two Ni atoms located at the corners—$x = 0.5$ b).

that the strong increase of atomic absorption takes place at this energy, we cannot observe very pronounced structure of the maximum B. The increase of DOS around 15 eV from FL (7132 eV at the edge) manifests itself in increase of the intensity at the top of the spectra and the increase of DOS around D results in disappearance of the minimum at 7136 eV but a minimum at 7133 eV is formed. In the DOS distribution for the model (b) we do not observe any increase of structures marked as B and C. The DOSs are distributed more uniformly over the whole energy range.

5. Summary

The electronic structure of ternary $Ni_3Al_{1-x}Fe_x$ alloys for two models of Fe-atom site occupancy was considered. The first model assumes that all Fe atoms are located at the cube corners in the fcc cell. The second model locates the Fe atoms at the centres of cube faces. The DOSs, over a wide energy range, were projected for all constituent atoms separately for different state symmetry. Additionally, the magnetic moments located at each atom and average magnetic moment per atom were calculated. The LMTO method of calculation was used for two models of the site occupancy. The results of calculations were compared with the appropriate x-ray spectra and with the average magnetic moment measured experimentally.

In the metallic alloys metallic bonds are formed and the changes introduced by these bonds in the DOS distribution are not as pronounced as in the ionic or ionic–covalent bonds.

The changes in DOS distribution for the considered models were found to be more pronounced at the Fe atom. The Fe and Ni atoms are very similar, therefore at sites of the Al atoms we did not observe significant changes after introducing Ni atoms into the cube corners. At the sites of Ni atoms, the differences for two models in DOS distribution were noticeable only in the d + s valence state distribution. Comparison of DOS with the x-ray spectra did not indicate any structure in the spectra which would favour the second model of Fe occupancy. The values of average magnetic moments calculated for the first model were also closer to the experimental values than those of the second model.

Direct comparison of changes in the DOS distribution of Ni_3Al after introduction of Fe

atoms with the changes observed in the x-ray spectra confirms predictions of the theory. One of the most general tendencies observed in the DOS distribution in ternary alloys at the Ni states which dominated in the total DOS was the disappearance of sharp, well localized peaks. Therefore, the DOS in ternary alloys is more uniformly distributed in energy space. This may be responsible for the increase of plasticity in Ni_3Al alloy after introducing iron.

The most surprising result of the calculation of magnetic moments located at the constituent atoms was the increase of the moment located at Ni atoms with the increase of Fe content. Such an effect has already been observed in the $(Fe_{1-x}Ni_x)_4N$ compound where Ni is also located at the faces of the cubic structure. To conclude consideration of the electronic structure for the two models of site occupancy of the Fe atoms in Ni_3Al ordered alloys and a comparison with x-ray spectra gave additional arguments in favour of the Fe atoms being located in the corners of the fcc cube.

Acknowledgments

This work was supported in part by grant No 2P03B 101 14 of the State Committee for Scientific Research (Republic of Poland). The authors would like to thank Dr P Laggard (LURE), Dr M Tischer (HASYLAB), Dr L-C Duda (Uppsala University) and Dr R Perera (ALS) for help in the performance of spectrum measurements.

References

[1] Pope D P and Ezz S S 1984 *Int. Metall. Rev.* **29** 136
[2] Suzuki T, Oya Y and Wee D M 1980 *Acta Metall.* **28** 301
[3] Takasugi T and Izumi O 1985 *Acta Metall.* **33** 1259
[4] Pascarelli S, Boscherini F, Mobilio S, Lawniczak-Jablonska K and Kozubski R 1994 *Phys. Rev.* B **49** 14 984
[5] Balasubramanian M, Lyver R, Budnick J I and Pease D M 1997 *Appl. Phys. Lett.* **71** 330
[6] Sluiter M H F and Kawazoe Y 1995 *Phys. Rev.* B **51** 4062
[7] Guard R W and Westbrook J H 1959 *Trans. AIME* **215** 807
[8] Fletcher G C 1971 *Physica* **56** 173
[9] Fletcher G C 1972 *Physica* **62** 41
[10] Hackenbracht D and Kubler J 1980 *J. Phys. F: Met. Phys.* **10** 427
[11] Xu Jian-hua, Miu B I, Freeman A J and Oguchi T 1990 *Phys. Rev.* B **41** 5010
[12] Iotova D, Kioussis N and Lim S P 1996 *Phys. Rev.* B **54** 14 413
[13] Reinmuth J, Passek F, Petrov V N and Donath M 1997 *Phys. Rev.* B **56** 12 893
[14] Muller P A, Singh D J and Silcox J 1998 *Phys. Rev.* B **57** 8181
[15] Morinaga M, Yukawa N and Adachi H 1984 *J. Phys. Soc. Japan* **53** 653
[16] Skriver H L 1984 *The LMTO Method* (Berlin: Springer)
[17] Shindo D, Kikuchi M, Hirabayashi M, Hanada S and Izumi O 1988 *Tran. Japan. Inst. Met.* **29** 956
[18] Efthimiadis K G, Antonopoulos J G and Tsoukalas I A 1989 *Solid State Commun.* **70** 903
[19] Efthimiadis K G and Tsoukalas I A 1993 *Solid State Commun.* **85** 81
[20] de Boer F R, Schinkel C J, Biesterbos J and Proost S 1969 *J. Appl. Phys.* **40** 1049
[21] Kong Y and Li F 1998 *Phys. Rev.* B **57** 970
[22] Azaroff L V (ed) 1974 *X-ray Spectroscopy* (New York: McGraw-Hill)
[23] Nordgren J, Bray G, Cramm S, Nyholm R. Rubensson J-E and Wassdahl N 1989 *Rev. Sci. Instrum.* **60** 1690
[24] Underwood J H, Gullikson E M, Koike M, Batson P C, Denham P E and Stele R 1996 *Rev. Sci. Instrum.* **67** 1
[25] Nagel D J, Papaconstantopoulos D A, McCaffrey J W and Criss J W 1973 *Proc. Int. Symp. X-Ray Spectra and Electronic Structure of Matter* ed A Faessler and G Wiech (Munich) p 51
[26] Lawniczak-Jablonska K, Inoue J, Tohyama T and Czyzyk M T 1994 *Phys. Rev.* B **49** 14 165
[27] Czyzyk M T, Lawniczak-Jablonska K and Mobilio S 1992 *Phys. Rev.* B **45** 1581
[28] Lawniczak-Jablonska K, Duda L-C, Guo J, Butorian S and Nordgren J 1996 *Physica* B **217** 78